Acta Cryst. (1974). A30, 251

High-Resolution Microscopy of Nonstoichiometric $Nb_{22}O_{54}$ Crystals: Point Defects and Structural Defects

BY S. IIJIMA*

Department of Physics, Arizona State University, Tempe, Arizona 85281, *U.S.A.*

AND S. KIMURA AND M. GOTO

National Institute for Researches in Inorganic Materials, Ibaraki, Japan

(*Received* 1 *October* 1973; *accepted* 22 *October* 1973)

With the use of high-resolution electron microscopy, defects have been observed in crystals of $Nb_{22}O_{54}$: two types of point defects and extended Wadsley-type defects having a structure corresponding to $Nb_{12}O_{29}$. For one type of point defect a model is proposed which contains two displaced metal atoms and two interstitial oxygen atoms within a 'block'. For the other, one metal atom and three oxygen atoms are considered to be missing from a tetrahedral site. Contributions made by the three types of defects to the non-stoichiometry of the crystals are discussed.

Introduction

It has been hitherto found that five compounds, namely $Nb_{12}O_{29}$, $Nb_{22}O_{54}$, $Nb_{47}O_{116}$, $Nb_{25}O_{62}$ and $Nb_{53}O_{132}$, exist in a composition range between NbO_2 and Nb_2O_5 (Norin, 1963, 1965; Gruehn & Norin, 1967, 1969; Roth & Wadsley, 1965). All compounds appearing in this composition range, except for NbO_2, are closely related and based on the ReO_3 structure, having double 'crystallographic shear planes' as essential constituents of their crystal structures (Wadsley & Andersson, 1970). These compounds are called 'homologous series compounds' or block structures, for they are known to belong to series represented by the general formulas, $M_{3n}O_{8n-3}$ and $M_{3n+1}O_{8n-2}$.

The conditions for stable existence of Magnéli-phase oxides in the system NbO_2–Nb_2O_5 at 1300 °C were studied by Schäfer, Bergner & Gruehn (1969) by using a H_2O/H_2 gas mixture and those at 1300 °C and 1400 °C by Kimura (1973) by using a CO_2/H_2 gas mixture. These experimental results show that the Magnéli-phase oxides, except for $Nb_{12}O_{29}$, have real compositions which deviate toward the oxygen deficient side, as shown in Fig. 1.

Allpress (1969, 1970) studied defect structures of a series of compounds in the system TiO_2–Nb_2O_5 by electron microscopy and suggested that the deviations from the crystallographically expected values may be attributed to Wadsley intergrowth defects, or microdomain intergrowths of neighbouring phases. Afterwards, Allpress & Roth (1971) found that Wadsley defects tend to disappear from compounds in the system WO_3–Nb_2O_5 during prolonged annealing. They concluded that Wadsley defects could not sufficiently explain the discrepancy in the observed compositions from an ideal structure in this system and that there could be some anion vacancies or metal interstitials contributing to oxygen deficiency of these compounds. Furthermore, Kimura (1973) proposed, after a thermodynamic calculation, that Wadsley defects may not be a predominant factor of nonstoichiometry of $Nb_{22}O_{54}$ and $Nb_{25}O_{62}$. Nimmo & Anderson (1972) found that no Wadsley defects were observable in the Nb_2O_5 phase at compositions down to at least $NbO_{2.495}$. They suspected that the occurrence of point defects, probably oxygen vacancies, in 'block' structures is favoured. One of the interests in studying Nb binary or ternary oxides systems is to determine whether Wadsley defects are the means of accommodating the deviation of a composition from stoichiometry and if not, what other types of defects are associated with the nonstoichiometry.

With careful use of high-resolution microscopy, approximate crystal-structure determinations, observations of both linear and planar defects occurring at the unit-cell level, and observation of point defects to some extent have been successfully carried out (Iijima & Allpress, 1974*a*, *b*). These achievements are based on the fact that two-dimensional lattice images taken under certain optimum conditions reflect the electrostatic potential distribution of crystals projected along the incident electron beam direction.

Using this technique we have previously reported (Iijima, Kimura & Goto, 1973) that point defects were observable in oxygen-excess samples of $Nb_{12}O_{29}$ in which tetrahedrally coordinated metal atoms are not present as essential constituents. After observing the annealing effect due to electron irradiation on these point defects, we proposed a model for the point defects. The density of the point defects was in agreement with that expected from the chemically analyzed composition of the samples.

In the present study, we examined several samples of

* On leave from the Research Institute for Scientific Measurements, Tohoku University, Sendai, Japan.

$Nb_{22}O_{54}$ with slightly different compositions by high-resolution electron microscopy, in the hope that we could find evidence for features providing an interpretation of its narrow range of homogeneity observed in the phase diagram (see Fig. 1). As a result, two different types of point defects have been observed as well as Wadsley defects. Their contributions to the nonstoichiometry of $Nb_{22}O_{54}$ will be discussed.

Experimental

The samples of $Nb_{22}O_{54}$ with nonstoichiometric compositions (black in color) were chosen from the collections prepared for the study of the phase equilibrium of NbO_2–Nb_2O_5 system by Kimura (1973). Their measured compositions were NbO_x ($x=2{\cdot}441$, 2·444, 2·446, 2·452 and 2·460). For the ideal composition, $x=2{\cdot}454$. They were obtained by oxidizing NbO_2 or reducing Nb_2O_5 at 1400 °C for 15–70 h by using a CO_2/H_2 gas mixture. It has been known in the previous phase identifications for these samples by X-ray analysis that the sample of $NbO_{2\cdot444}$ showed a minor amount of the $Nb_{12}O_{29}$ and the $NbO_{2\cdot460}$ a trace of $Nb_{47}O_{116}$.

Samples were ground in an agate mortar and fine fragments from the samples were collected on holey-carbon supporting films. Very thin crystals were chosen and examined by an electron microscope at 100 kV, as described previously (Iijima, 1973). Both electron-microscope images and electron diffraction patterns were recorded from more than 20 fragments from each sample. To reduce the electron irradiation effect during the observation, the specimens were observed as quickly as possible at a minimum intensity of the electron beam.

Results and interpretation

The crystal structure of $Nb_{22}O_{54}$ [Fig. 2(*a*)] has been known as the homologue having $n=7$ in a series with the general formula $Nb_{3n+1}O_{8n-2}$ and is closely related to H-Nb_2O_5 ($n=9$) (Gatehouse & Wadsley, 1964). Each square represents an octahedron of a simple ReO_3 structure. Two kinds of blocks, shown by dark and light squares, are centered about the two levels perpendicular to the b axis and are 1·9 Å apart. At one level, the blocks have the dimensions 3×4, and are joined by octahedral edge-sharing, to form separated, stepped rows. At the other level the blocks are 3×3, and are separated by Nb atoms in tetrahedral sites. The 3×3 and 3×4 blocks are joined by sharing their common edges which form crystallographic shear planes. A simple representation of the same structure is shown in Fig. 2(*b*), in which each block of octahedra is drawn as a rectangle. The unit cell (outlined in the models) has the dimensions $a=21{\cdot}2$, $b=3{\cdot}82$, $c=15{\cdot}6$ Å and $\beta=124{\cdot}5°$.

A two-dimensional lattice image of $Nb_{22}O_{54}$ viewed down the short b axis [Figs. 3(*b*), 10] shows a contrast distribution similar to the *ac*-plane projection of the structure of the crystal. The channels containing Nb atoms are imaged as white dots, the regions where the octahedra share their edges, or shear planes, show grey contrast and the region near a tetrahedrally coordinated metal atom, surrounded with eight metal atoms in the nearest octahedra, is black.

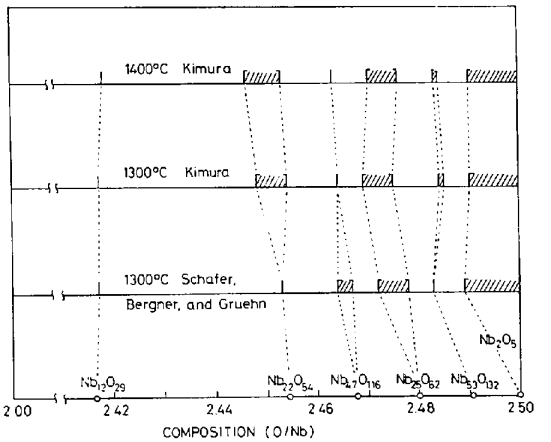

Fig. 1. Real compositions of the niobium oxides under equilibrium with various atmospheres, determined by Schäfer, Bergner & Gruehn (1969) and Kimura (1973).

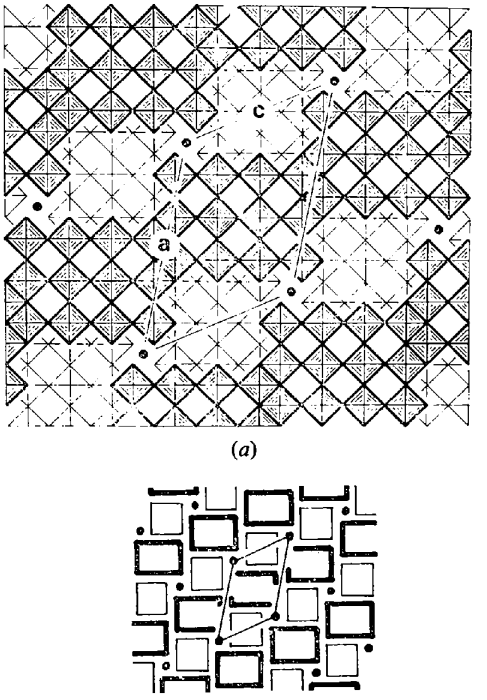

(*a*)

(*b*)

Fig. 2. (*a*) Idealized structure of $Nb_{22}O_{54}$ and (*b*) its simple representation. The darker and lighter squares represent octahedra of NbO_6 which form 3×3 and 3×4 blocks by their corner sharing. They are centered about the two levels perpendicular to the b axis and are 1·9 Å apart. Black circles represent tetrahedrally coordinated Nb atoms. The unit cell in projection is outlined ($a=21{\cdot}2$, $b=3{\cdot}82$, $c=15{\cdot}6$ Å and $\beta=124{\cdot}5°$).

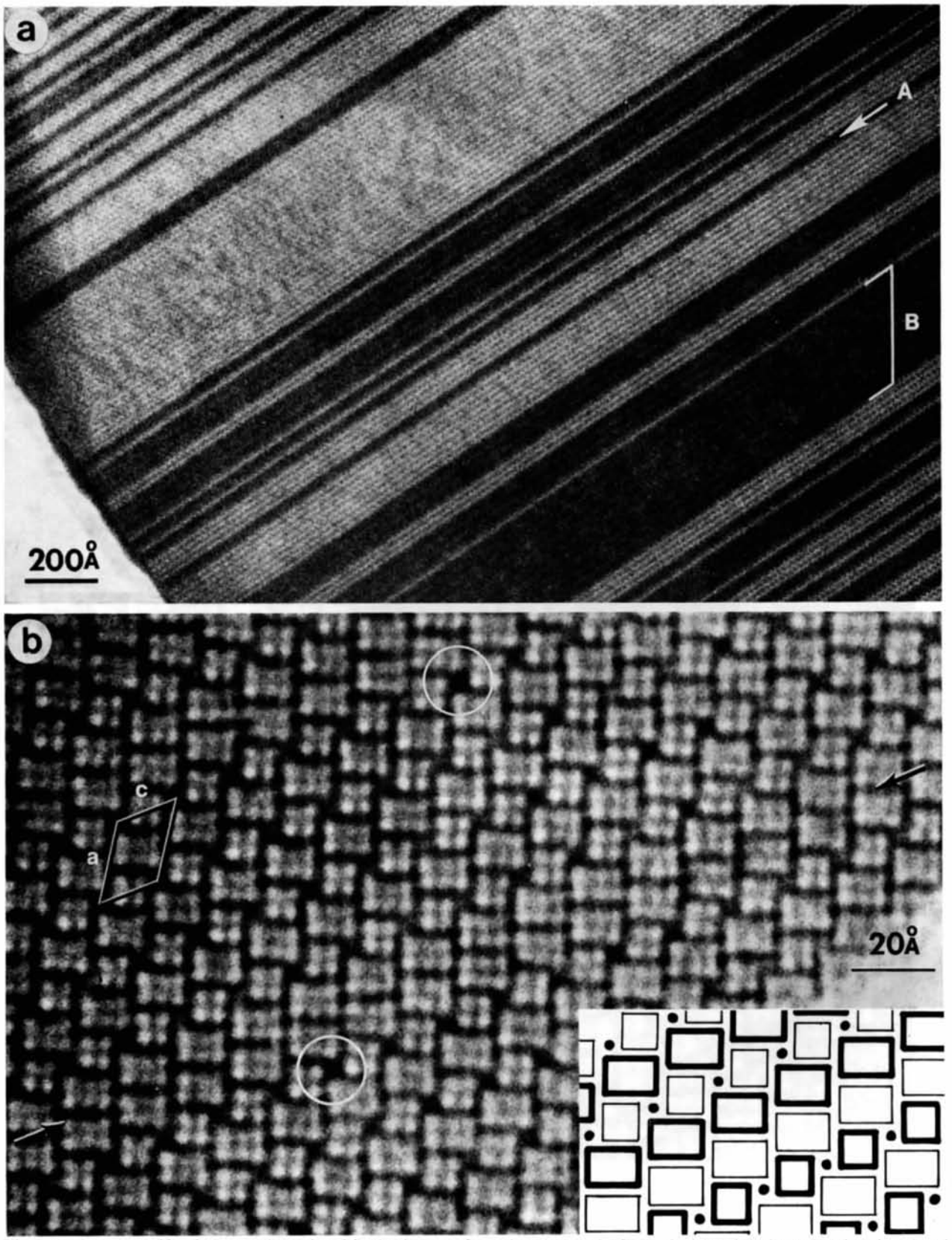

Fig. 3. (*a*) Low-magnification two-dimensional lattice image of a reduced crystal of $Nb_{22}O_{54}$ showing the ordered region (grey) and the Wadsley defects (diagonally running black bands). (*b*) High-magnification lattice image showing the $Nb_{12}O_{29}$-type Wadsley defect (indicated by arrows) which corresponds to the black bands indicated by *A* in Fig. 3(*a*). Some of the tetrahedral sites show darker contrast than the others, suggesting metal-atom vacancies.

[*To face p.* 252

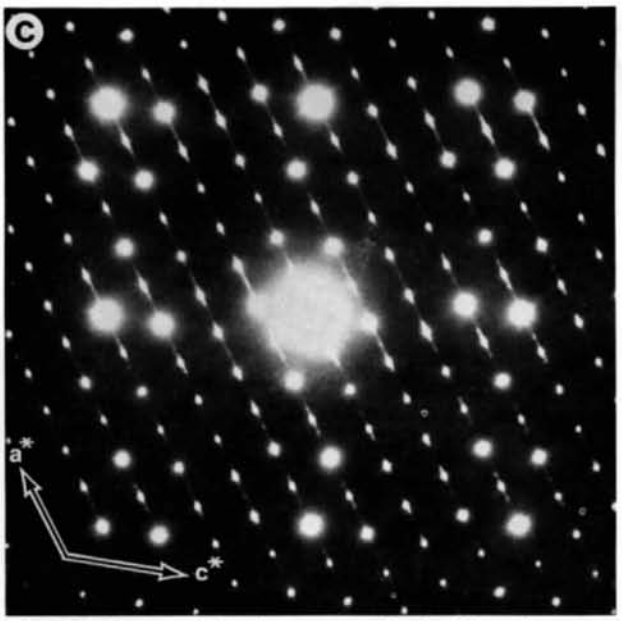

Fig. 3. (*c*) Electron diffraction pattern obtained from the crystal of $Nb_{22}O_{54}$ containing $Nb_{12}O_{29}$-type Wadsley defects.

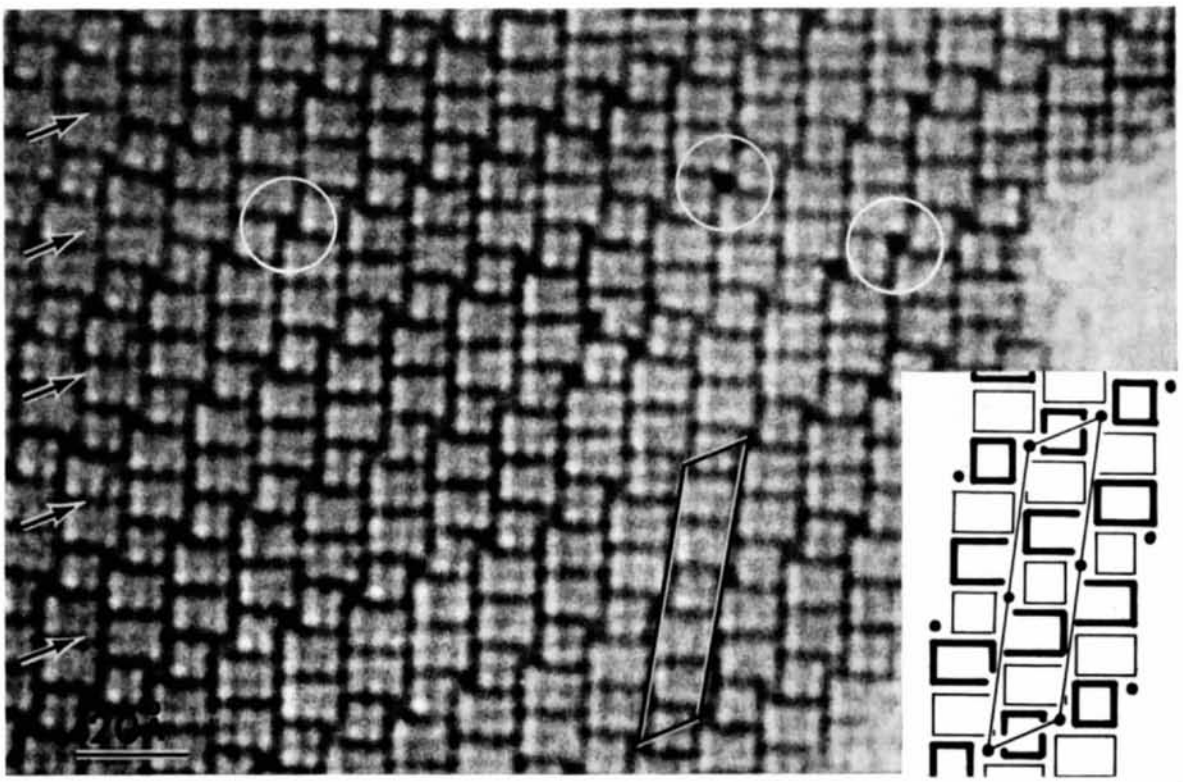

Fig. 4. An ordered intergrowth of the $Nb_{12}O_{29}$-type Wadsley defects (indicated by arrows) into the host structure which corresponds to the region shown by *B* in Fig. 3(*a*). This region forms a superstructure having a composition of $Nb_{34}O_{83}$. The unit cell is outlined.

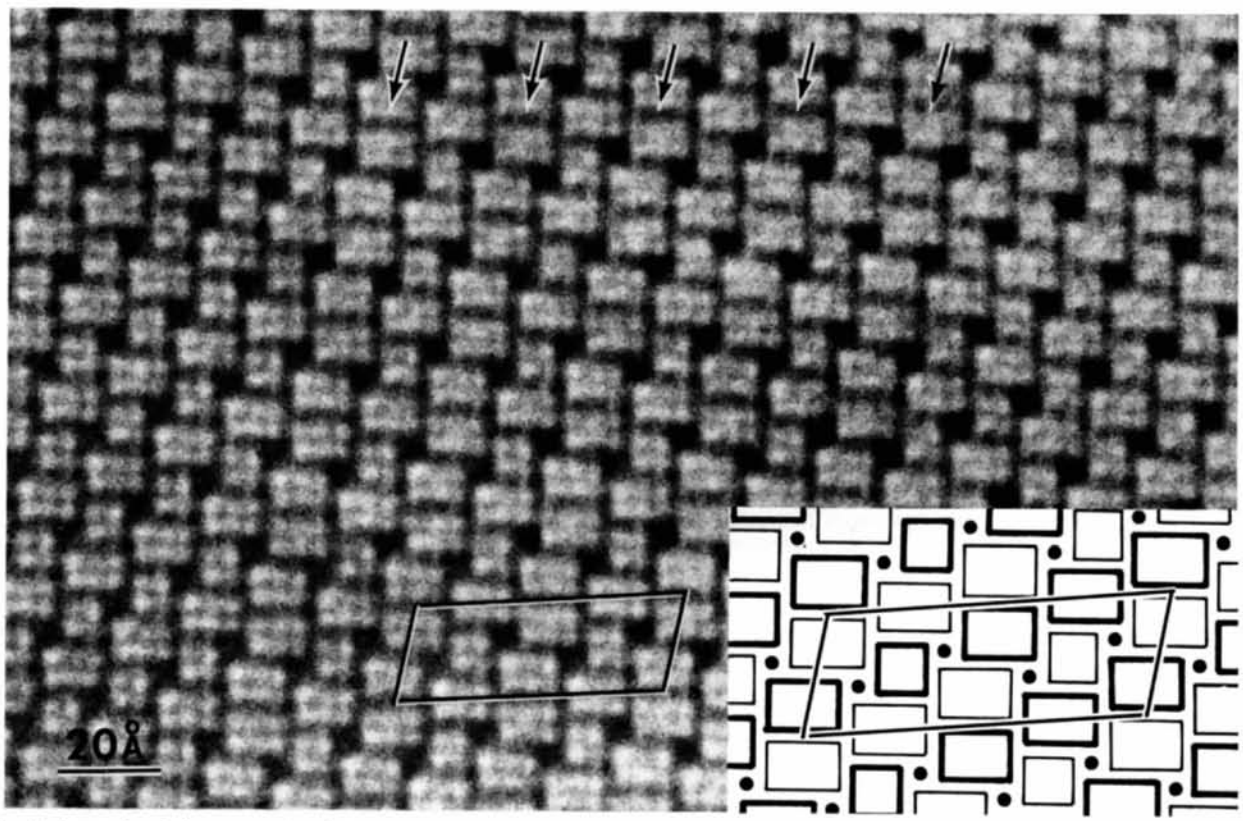

Fig. 5. An ordered intergrowth of the $Nb_{25}O_{62}$-type Wadsley defects (indicated by arrows) into the host structure. The region forms a superstructure having a composition of $Nb_{47}O_{116}$. The unit cell is outlined.

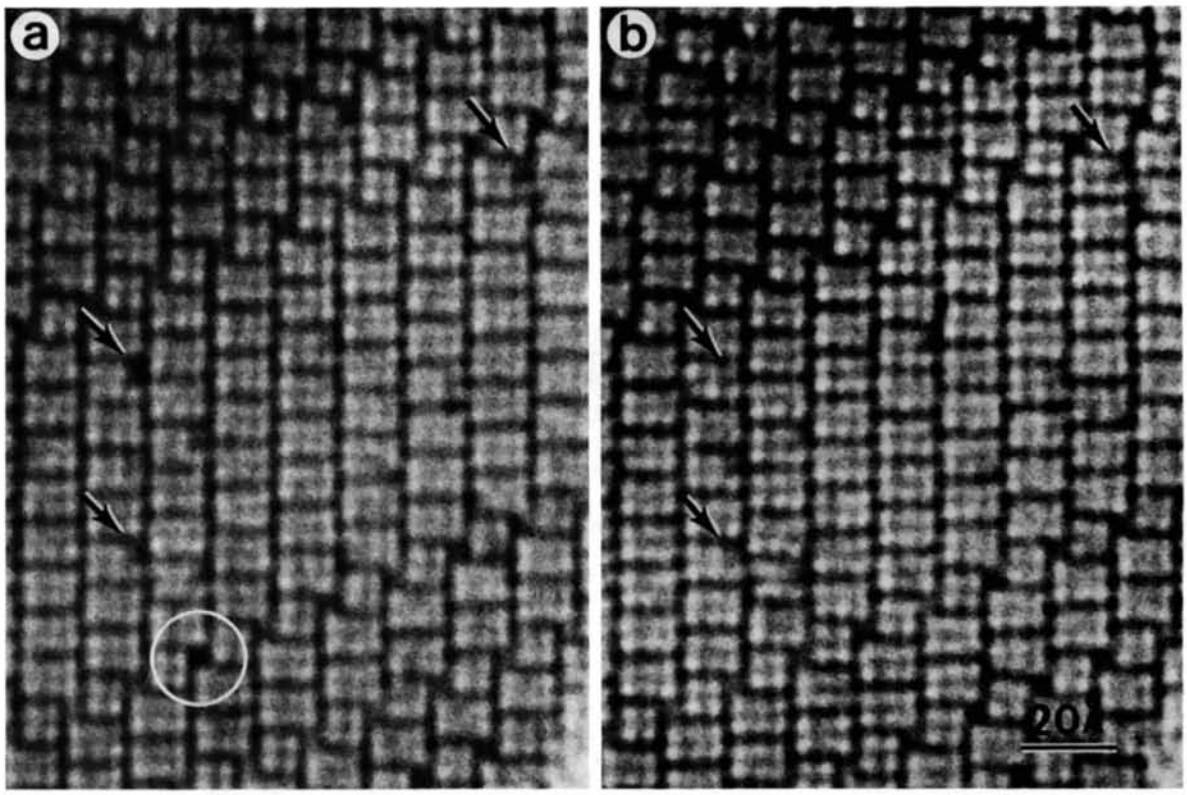

Fig. 6. (*a*) A micro-domain of a monoclinic phase of $Nb_{12}O_{29}$ found in a fragment of the reduced $Nb_{22}O_{54}$. The domain contains black spots within 3×4 blocks (arrowed), indicating the presence of point defect complexes of interstitials at those positions. (*b*) The same microdomain imaged after an electron beam irradiation for several minuites. Note the black spots appearing in Fig. 6(*a*) have disappeared.

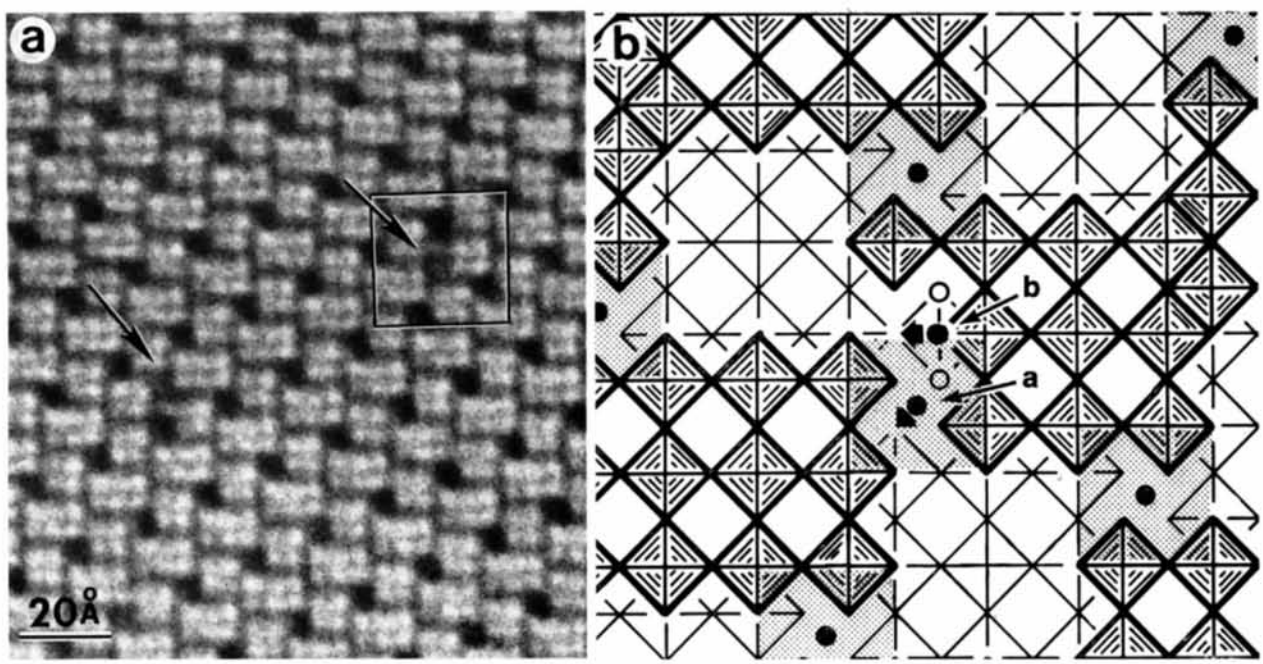

Fig. 7. (*a*) Black spots (arrowed) appearing in an ordered region of a reduced crystal of $Nb_{22}O_{54}$, resembling those observed in a domain of $Nb_{12}O_{29}$ shown in Fig. 6(*a*). (*b*) A proposed octahedral model for the black spot. The defect is a point defect complex composed of two displaced metal atoms (indicated by *a* and *b*) and two oxygen atoms (open circles). The metal atom (labeled *a*) has a tetrahedral coordination which is similar to those present in the host structure (shaded).

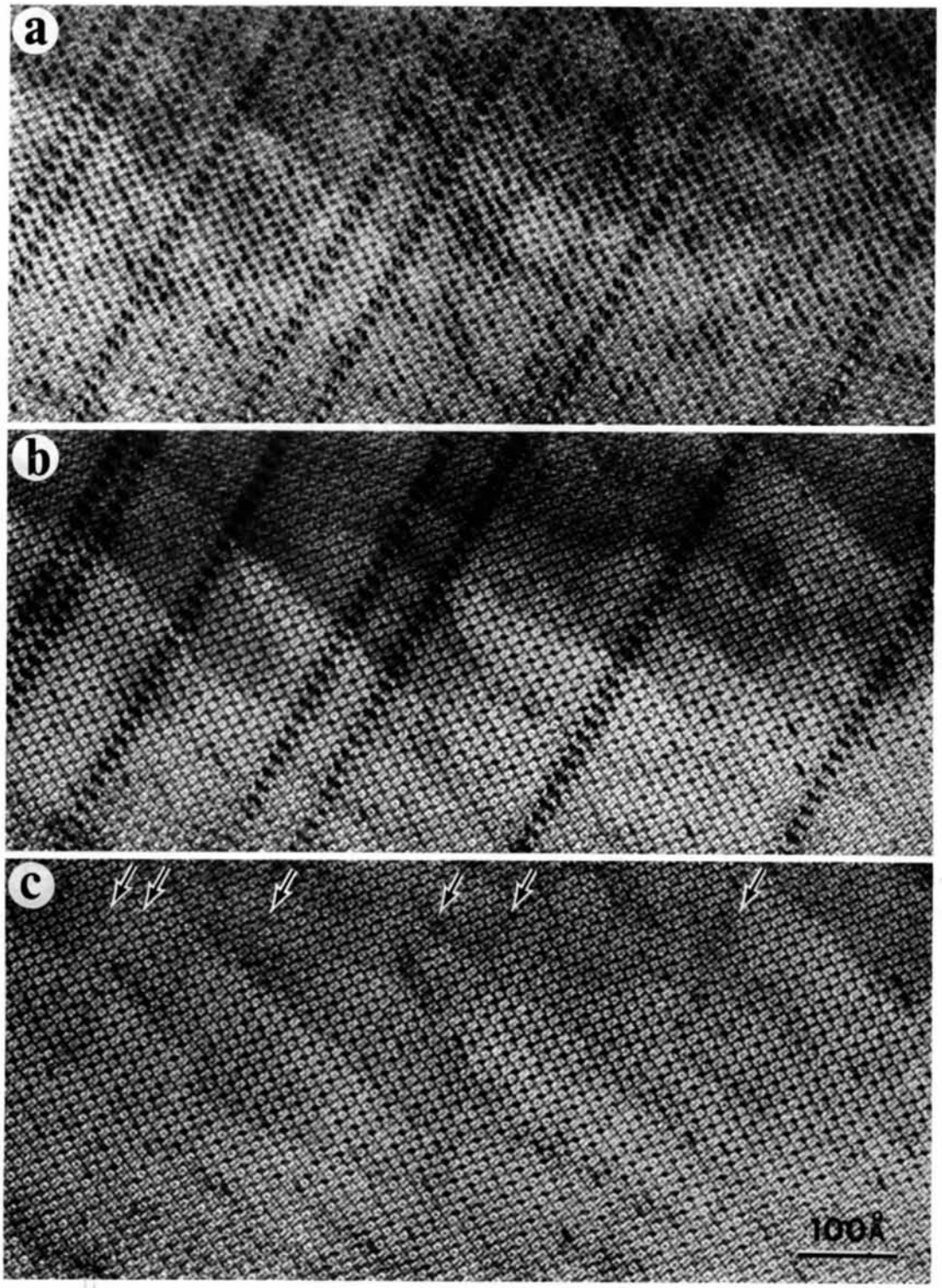

Fig. 8. A series of pictures at a relatively low magnification showing the effects of electron-beam irradiation on the point-defect complexes. (*a*) At a very early stage of the irradiation. (*b*) After several minutes irradiation. (*c*) After intense irradiation achieved by taking out the condenser aperture of the microscope. The $Nb_{12}O_{29}$-type Wadsley defects are indicated by arrows.

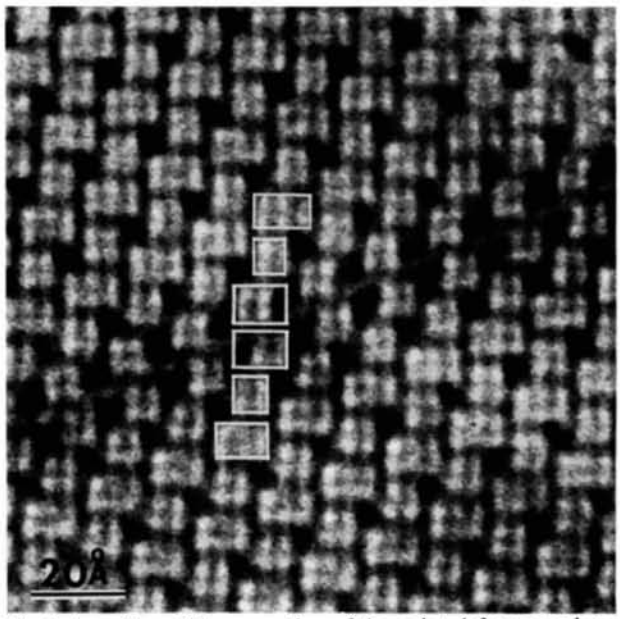

Fig. 9. A preferential aggregation of the point-defect complexes at the boundary between the $Nb_{12}O_{29}$-type Wadsley defect and the host lattice.

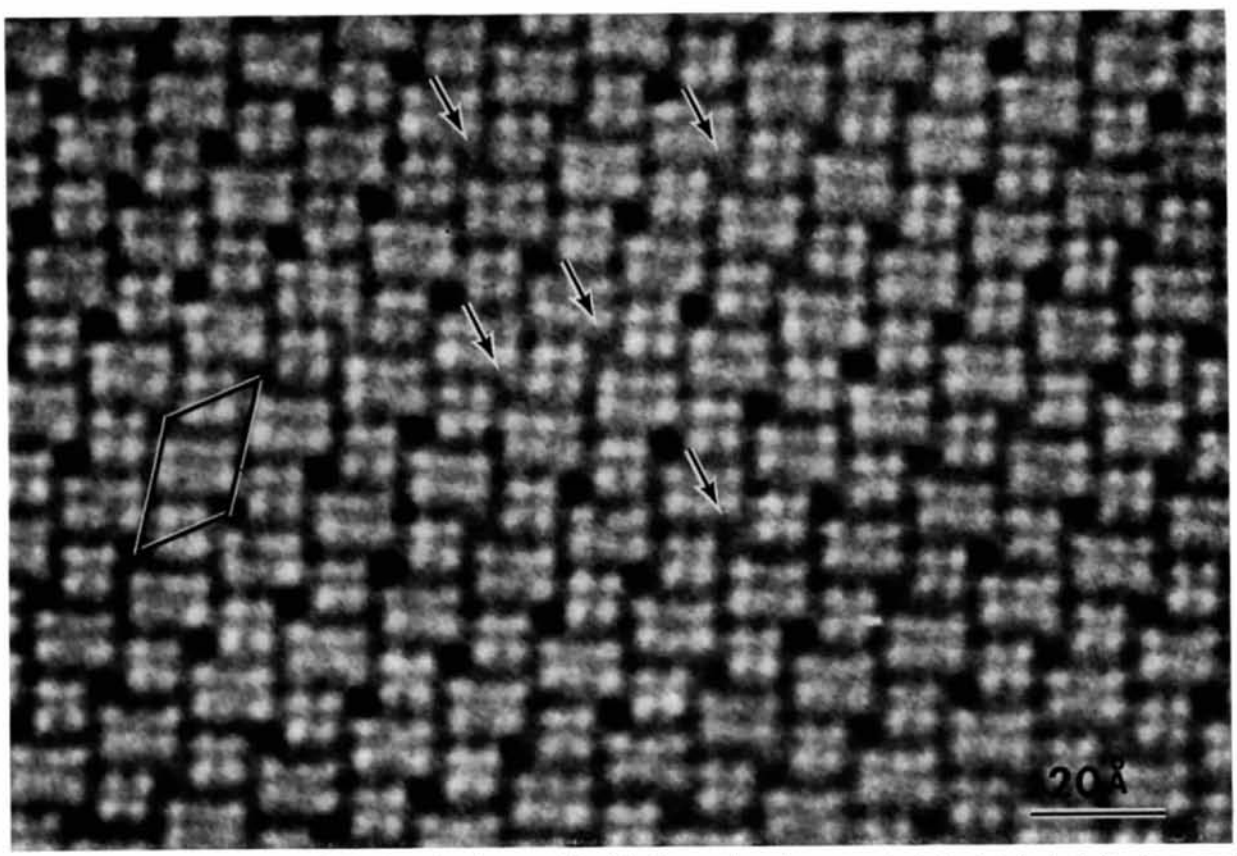

Fig. 10. The image of fragment of $Nb_{22}O_{54}$, showing considerable fluctuations in contrast at the tetrahedral sites in a matrix of $Nb_{22}O_{54}$. This suggest that the sites with lighter contrast (arrowed) contain metal-atom vacancies.

The appearance of the image contrast is quite dependent on the focusing of the microscope, crystal thickness and orientation. A good correspondence of the image with the crystal structure could be obtained only by satisfying thoroughly these critical conditions. In particular, for investigation of point defects the crystals should be imaged after setting the crystal orientation parallel to the *b* axis with accuracy of 2×10^{-3} rad. All images were taken from the *b*-axis orientation of the crystals.

Wadsley defects

Fig. 3(*a*) shows a relatively low-magnification image of a fragment of $NbO_{2\cdot441}$, indicating some planar defects (black bands). A high-magnification image of a region similar to that indicated by *A* is shown in Fig. 3(*b*). The regular alternation of the rows of 3×3 and 3×4 blocks in an ordered region is upset at the positions indicated by arrows, in which two rows of the 3×4 blocks adjoin. This is illustrated in the inset. The defect region intergrows coherently parallel to both *c* and *b* axes of the host lattice of $Nb_{22}O_{54}$ and consists of structural components of $Nb_{12}O_{29}$ which is the neighbouring phase to $Nb_{22}O_{54}$ having less oxygen content. Note that almost all these defect layers, Wadsley defects, are extended two-dimensionally (perpendicular to the page) and never terminate within a crystal. The electron diffraction pattern taken from the fragment containing these Wadsley defects is shown in Fig. 3(*c*). The main spots are due to the host lattice of $Nb_{22}O_{54}$ and the streaks parallel to the a^* axis are consistent with the occurrence of the observed Wadsley defects.

It was found that these Wadsley defects have a tendency to appear in pairs or in groups with a regular spacing [indicated by *B* in Fig. 3(*a*)] in a matrix lattice. An example is shown in Fig. 4, in which the Wadsley defects are indicated by arrows. The faulted region forms an ordered intergrowth, namely a superstructure, consisting of alternating layers of $Nb_{12}O_{29}$ and $Nb_{22}O_{54}$ parallel to the *c* axis of the $Nb_{22}O_{54}$ structure. The unit cell, indicated in the inset, has dimensions of roughly $a=62\cdot4$, $b=3\cdot8$, $c=15\cdot6$ Å and $\beta=120°$. The composition is $Nb_{34}O_{83}$ ($=NbO_{2\cdot441}$). These microdomains of the superstructure did not grow more than about 15 unit cells wide.

Occurrences of these Wadsley defects (hereafter called $Nb_{12}O_{29}$-type Wadsley defects) will make the overall composition of the specimen oxygen deficient. They were very common in fragments from all samples examined here except for $NbO_{2\cdot460}$. There was a general tendency for samples with higher degree of oxygen deficiency to contain higher concentrations of the $Nb_{12}O_{29}$-type Wadsley defects. This supports qualitatively the idea that the deviation in composition toward the oxygen deficiency from the ideal value is accommodated by coherent intergrowths of the lower Nb oxides of $Nb_{12}O_{29}$.

In order to answer the further question, whether the Wadsley defects are the only means of accommodating the deviation of the composition of the reduced samples of $Nb_{22}O_{54}$ from stoichiometry, the concentration of the Wadsley defects was examined in numerous photographs taken from 25 fragments from the sample of $NbO_{2\cdot446}$. For this purpose, it has been confirmed that the fragments from this sample did not contain any other predominant Wadsley defects except for the $Nb_{12}O_{29}$-type ones. The other samples were not examined because some of the fragments from $NbO_{2\cdot441}$ and $NbO_{2\cdot444}$ showed only the $Nb_{12}O_{29}$ phase or small domains of it and fragments from $NbO_{2\cdot452}$ and $NbO_{2\cdot460}$ showed $Nb_{25}O_{62}$-type Wadsley defects or domains of the higher oxide phase $Nb_{47}O_{116}$, which will be described later. The existence of these defects will make the interpretation difficult.

The results showed that 554 fringes of $Nb_{12}O_{29}$-type Wadsley defects were counted for 5790 fringes corresponding to the *a*-axis spacing of the matrix lattice of $Nb_{22}O_{54}$. From these values, assuming that the deviation in composition from the ideal value (2·454) would be accommodated only by occurrences of the $Nb_{12}O_{29}$-type Wadsley defects, we estimated the metal–oxygen ratio of the sample to be $NbO_{2\cdot452}$. This is much higher than the chemically analyzed value 2·446. This suggests that it is insufficient to explain the nonstoichiometry of the sample only in terms of the Wadsley defects. It will be expected, therefore, that reduced samples of $Nb_{22}O_{54}$ should contain some kinds of point defects contributing to oxygen deficiency.

There was another type of Wadsley defect containing structural components similar to the $Nb_{25}O_{62}$ phase. This is shown by arrows in Fig. 5. Such defects were observed in the fragments from the sample of $NbO_{2\cdot452}$ whose composition is the closest to the ideal formula $Nb_{22}O_{54}$ among the oxygen deficient samples. The faulted region forms a small domain of the $Nb_{47}O_{116}$ phase ($=NbO_{2\cdot468}$) which has been known as the higher oxide phase next to $Nb_{22}O_{54}$ in the phase diagram (see Fig. 1). The inset shows the model for this structure and the unit cell is indicated. This type of Wadsley defect shifts the overall composition toward the oxygen excess but it occurred with such a low density that it could not contribute appreciably to the nonstoichiometry. It is noted that both oxygen-deficient and excess type Wadsley defects with respect to the ordered phase of $Nb_{22}O_{54}$ can coexist in this sample.

On the other hand, the $Nb_{47}O_{116}$ phase was predominant in the sample of $NbO_{2\cdot460}$ for which composition oxygen is in excess with respect to the ideal value of $Nb_{22}O_{54}$. About two thirds of the fragments from this sample showed only the $Nb_{47}O_{116}$ phase which contained small domains of $Nb_{22}O_{54}$ as intergrown layers. This is qualitatively consistent with the fact that the sample $NbO_{2\cdot460}$ has oxygen excess.

Point defect within a 'block'

Fig. 6(*a*) shows a small domain of a monoclinic phase of $Nb_{12}O_{29}$. Similar domains were observed often

in the samples of $NbO_{2.441}$ and $NbO_{2.444}$. It was found that these domains always contained black spots (arrowed) within a 3×4 block. Fig. 6(*b*) was taken after several minutes from the same region as shown in Fig. 6(*a*). It is obvious that the black spots have disappeared during the observation with an electron microscope. A similar observation has been made previously on the fragments from slightly oxygen-excess samples of $Nb_{12}O_{29}$ (Iijima, Kimura & Goto, 1973). Therefore, these black spots may result from the same origin and can be interpreted in a similar way.

In summary, they are due to the occurrence of the point-defect complexes composed of two displaced metal atoms and two interstitial oxygen atoms, giving a structure which is similar to the tetrahedral site present in $Nb_{22}O_{54}$. We called it a 'quasi-tetrahedral site'. It requires two extra oxygen atoms per one defect and thus contributes to the nonstoichiometry of oxygen excess of the specimen.

Similar black spots were also observed in the 3×4 blocks in ordered regions of $Nb_{22}O_{54}$ from all the samples except for $NbO_{2.460}$. An example of this taken from the fragment of $NbO_{2.446}$ is reproduced in Fig. 7(*a*). Black spots (arrowed) are located at the position corresponding to one of the 2×3 channels within a 3×4 block. By analogy with the defect appearing in the $Nb_{12}O_{29}$ region, a possible model for the black spot was derived which is illustrated in Fig. 7(*b*).

Fig. 8(*a*), (*b*), (*c*) shows a series of pictures taken successively at several minute intervals. The black bands represent $Nb_{12}O_{29}$-type Wadsley defects described previously. In the regions of $Nb_{22}O_{54}$ between those bands [Fig. 8(*a*)], there are many black spots, which have disappeared with exposure time [Fig. 8(*b*)]. The image in Fig. 8(*c*), which was recorded after an intense electron irradiation, performed by removing a condenser aperture of the microscope, does not contain black spots except at tetrahedral sites. Note that the black spots were preferentially formed at the boundary regions between the $Nb_{12}O_{29}$-type Wadsley defects and a matrix lattice of $Nb_{22}O_{54}$ [Fig. 8(*b*)]. A typical example is shown in Fig. 9. The black spots at the boundaries can also be explained by assuming the occurrence of the point defects described in Fig. 7(*b*). They are more stable under the electron irradiation than those in ordered regions but with intense electron-beam irradiation they have also disappeared as seen in Fig. 8(*c*), where the $Nb_{12}O_{29}$-type Wadsley defects are indicated by arrows. Therefore, these Wadsley defects have contained oxygen excess before the electron irradiation and after releasing the oxygen they seem to become stoichiometric structures.

The fact that these defects were easily annealed out under electron irradiation makes the quantitative interpretation of the nonstoichiometry of the present samples difficult. It can be said, nevertheless, that the density of these point defects [Fig. 8(*a*)] seems to be high enough to contribute to the oxygen excess of the specimen, as in the $Nb_{12}O_{29}$.

Point defect at a tetrahedral site

The most interesting finding in this study is that there are considerable fluctuations in contrast at the tetrahedral sites in a matrix of $Nb_{22}O_{54}$. This can be clearly seen in an image of a fragment from $NbO_{2.452}$ shown in Fig. 10 and also in Figs. 3(*b*), 4, 6(*a*), in which some of tetrahedral sites are darker (circled) or lighter (arrowed). The fluctuation was observable only in a very thin region of the crystal. In a previous observation by Iijima (1973) on H-Nb_2O_5 with stoichiometric composition, which also has tetrahedral sites, no observable differences in the contrast among those sites were visible. Thus it is unlikely that the differences are due to some artifacts during the observation, such as contamination on the specimen.

From the theory of the image contrast (Cowley & Iijima, 1973), if the crystal is about 10 Å thick for a heavy-atom crystal, the image contrast can be interpreted in terms of a weak phase object and is linearly proportional to the projected crystal potential along the incident beam direction. An intuitive interpretation of the observed fluctuation in the contrast, therefore, is that some of the tetrahedrally coordinated metal atoms are absent from their positions; *i.e.* there are metal-atom vacancies. This is illustrated in Fig. 11(*b*), compared with the model for a tetrahedrally coordinated metal atom (hereafter represented by Nb_{IV}) shown in Fig. 11(*a*). The frame of the nearest neighbouring oxygen ions in a vacant site of Nb_{IV} is unchanged. It is obvious that this defect structure is electrostatically unfavourable. Furthermore, since this defect structure has an oxygen excess, this will be in conflict with the fact that our reduced samples should be oxygen deficient.

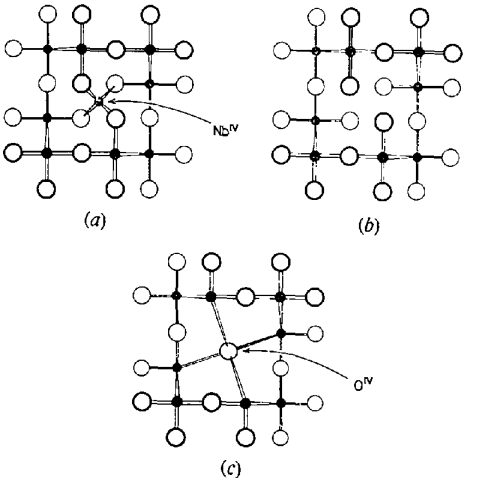

Fig. 11. A proposed model for the defect at the tetrahedral site appearing in Fig. 10. Black dots are niobium atoms and open circles oxygen atoms. (*a*) A normal tetrahedral site. (*b*) A postulated metal-atom vacancy at the tetrahedral site. (*c*) A presently proposed model, where NbO_4 at the tetrahedral site is substituted by a oxygen atom.

A proposed model for this defect is represented in Fig. 11(*c*).* The frame of oxygen ions in the vicinity of a vacant site of Nb_{IV} is perhaps destroyed and is replaced by one oxygen ion. This may possibly occur because the repulsive forces between the anions [in Fig. 11(*b*)] may reduce the stability of the crystal structure. Incidentally, it should be clear that the structures shown in Fig. 11 do not represent the reaction process for the formation of a vacant Nb_{IV} site. According to this model, when one Nb_{IV} atom is lost from the tetrahedral site, three oxygen atoms are also missing. It is a cluster of vacancies of one Nb and three oxygen atoms, expressed as NbO_3. Thus this type of point defect may contribute not to an oxygen excess but to an oxygen deficiency of the specimen. This is consistent with the fact that our samples are oxygen deficient with respect to the host lattice.

Discussion

The visualization of point defects by high-resolution microscopy has been proved to be possible. It has been shown directly for the first time that point defects play an important role in nonstoichiometry of the compounds of NbO_2–Nb_2O_5 system. Their presence had been expected but has never been observed before. It is obvious that the high-resolution lattice-imaging method has a great potential for the study of point defects as well as extended defects in solids.

Equilibrium of Wadsley defects

Our previous experiments on the quenched samples of 'block' structures of *H*-Nb_2O_5 and $TiO_2.7Nb_2O_5$ with stoichiometric or nonstoichiometric compositions (Iijima, 1973; Iijima & Allpress, 1973) showed several different types of Wadsley defects and/or relatively larger domains of phases different from the host structures. Their compositions were either oxygen-deficient or excess with respect to the host structures, and they often coexisted in the host lattices. It was suggested from those observations that the variety of planar defects probably resulted from the non-equilibrium state of the crystals. Such fluctuations in structure, occurring at the unit-cell level, have restricted the further arguments on nonstoichiometry of those crystals. For a better understanding of nonstoichiometry supposedly caused by the presence of Wadsley defects, therefore, it is required to use the well-equilibrated materials. In this sense, we believe that our samples from Kimura's (1973) experiment of phase equilibrium were satisfactorily characterized.

It was found that the most common Wadsley defect in the slightly reduced oxides of $Nb_{22}O_{54}$ was of the $Nb_{12}O_{29}$ type. The $Nb_{12}O_{29}$-type Wadsley defect has not been discussed in the previous literature (for instance, Anderson, 1970) probably because no observation of the existence of a range of composition for the $Nb_{22}O_{54}$ phase was reported until Kimura's study. This occurrence can be readily understood by extending the established concept of the Wadsley defects, *i.e.* coherent intergrowths of neighbouring phases into the host structure.

Of samples of $Nb_{22}O_{54}$ presently examined, the $NbO_{2.446}$ contained only one type of Wadsley defect, the $Nb_{12}O_{29}$-type, which was randomly distributed in the host lattice. However, some fragments from $NbO_{2.441}$ and $NbO_{2.444}$, having less oxygen content than the others and located close to the region of $Nb_{12}O_{29}$ phase in the phase diagram, frequently contained domains of $Nb_{12}O_{29}$ phase. The fragments from $NbO_{2.452}$ showed both $Nb_{12}O_{29}$-type and $Nb_{25}O_{62}$-type Wadsley defects but the fragments from $NbO_{2.460}$ showed no $Nb_{12}O_{29}$-type Wadsley defects but only $Nb_{25}O_{62}$-type defects and its ordered intergrowths. Note that in most samples only one type of Wadsley defect could be observed predominantly. It is of interest to compare this result with the previous observation on quenched samples. It seems that Wadsley defects are thermodynamically stable and only neighbouring phases of the host structure are allowed to be Wadsley defects in well-equilibrated materials.

The phase rule states that only a critical oxygen pressure can allow two solid phases to coexist in equilibrium in the binary system Nb–O. It is therefore understood that under the usual experimental conditions of equilibration, the niobium oxide specimen is expected to become eventually only one homogeneous phase. The observed occurrence of large domains of $Nb_{12}O_{29}$ in the $Nb_{22}O_{54}$ host matrix strongly suggests that the specimen is in the process of forming the $Nb_{22}O_{54}$ phase with homogeneously distributed $Nb_{12}O_{29}$-type Wadsley defects. Thus, the samples of $NbO_{2.446}$ have been satisfactorily equilibrated, while others have not. The reaction conditions (1400 °C, 15–27 h) for those samples probably have been insufficient for attaining equilibrium states. This agrees with the experiment by Allpress & Roth (1971). They showed that by annealing nonstoichiometric Ti–W oxides both the number of types of Wadsley defects and their densities were decreased but they were never entirely removed from the samples even after prolonged annealing.

Nonstoichiometry

As we have described in the preceding section, major defects in the crystals of $Nb_{22}O_{54}$ were $Nb_{12}O_{29}$-type Wadsley defects (oxygen deficient), point-defect com-

* Recently Anderson *et al.* (1973) studied the block structure of $GeNb_{18}O_{47}$, containing 3×3 blocks and tetrahedral sites and proposed a model for the point defect at the tetrahedral sites different from ours. Tetrahedral sites at $z=\frac{1}{4}$ and $\frac{3}{4}$ could be partially substituted by two octahedral sites at $z=0$ or $\frac{1}{2}$ and cations in these positions connect the blocks at the same level [see Fig. 2(*a*)]. If this is the case, these areas could be imaged darker than those without defects instead of lighter as for the present model because of higher electrostatic potential projected along the incident electron-beam direction. Therefore, the darker regions shown by circles in Figs. 3(*b*), 4 & 6(*a*) could result from such defects. To resolve this argument, the calculation of image contrast of the defects will be necessary.

plexes, or 'quasi-tetrahedral sites', containing interstitials within a block (oxygen excess) and point-defect complexes containing vacancies at tetrahedral sites (oxygen deficient). The nonstoichiometry of $Nb_{22}O_{54}$ phase, therefore, might result from net effects of those three defect types. These observations evidently gave an answer to the question whether Wadsley defects are the only means of accommodating the deviation of a composition from stoichiometry. The density of $Nb_{12}O_{29}$-type Wadsley defects in the fragments of the reduced $Nb_{22}O_{54}$ increases as the oxygen content in the samples decreases, indicating that Wadsley defects are undoubtedly associated with the nonstoichiometry of this phase. This has been confirmed somewhat quantitatively on the specimen $NbO_{2.446}$. The estimated density, however, was not high enough to accommodate the discrepancy of the composition from the measured value. In addition to this, it was found that point-defect complexes of interstitials contributed to the oxygen excess of the reduced materials. This means that the net effects of the point defects on the composition must be a further decrease in oxygen excess. As a result, we should conclude that the point-defect complexes of NbO_3 vacancies play a significant role in the nonstoichiometry of the $Nb_{22}O_{54}$ phase.

We believe that this type of point defect will be a common defect in nonstoichiometric oxides of Nb having Nb_{IV} sites. This is likely because the narrow ranges of homogeneity in the NbO_2–Nb_2O_5 system are mainly observed in the structures having Nb_{IV}, and $Nb_{12}O_{29}$, which does not have such sites, does not show an appreciable deviation from the ideal composition. The more the crystal incorporates the vacant sites of Nb_{IV}, the more its composition will shift toward the oxygen-deficient side, losing more oxygen atoms than niobium atoms. In this way the oxygen-deficient compositions of the $Nb_{22}O_{54}$, $Nb_{25}O_{62}$ and $Nb_{28}O_{70}$ (H-Nb_2O_5) phases can be fully interpreted. For reference, a simple calculation was carried out to obtain the compositions of those phases when all the tetrahedral Nb atoms are absent from their sites. The result is shown below:

(a) $Nb_{22}O_{54}$ ($NbO_{2.454}$) with no Nb_{IV}: $NbO_{2.429}$
(b) $Nb_{25}O_{62}$ ($NbO_{2.480}$) with no Nb_{IV}: $NbO_{2.458}$
(c) $Nb_{28}O_{70}$ ($NbO_{2.500}$) with no Nb_{IV}: $NbO_{2.482}$.

According to Kimura's (1973) experiment the most oxygen-deficient compositions of $Nb_{22}O_{54}$, $Nb_{25}O_{62}$ and $Nb_{28}O_{70}$ at 1400 °C are $NbO_{2.446}$, $NbO_{2.470}$ and $NbO_{2.490}$ respectively. Thus the effect of the absence of Nb_{IV} is found to be enough to cover the observed deviations in compositions.

Point defects and Wadsley defects

In the process of considering the phase transformation from $Nb_{22}O_{54}$ into $Nb_{12}O_{29}$, or *vice versa*, two important observations have been made on the point defect complexes of interstitials, or 'quasi-tetrahedral sites' present in crystals of reduced $Nb_{22}O_{54}$, *i.e.* the defects are more slowly annealed out by electron-beam irradiation than those randomly distributed in the host lattice and they aggregate preferentially at the boundaries between $Nb_{12}O_{29}$-type Wadsley defects and the host structure [Fig. 9(a)]. The elimination of the 'quasi-tetrahedral sites' will involve diffusion of oxygen ions or oxygen vacancies through the host lattice. Although such an elimination of the point defects took place under the electron-beam irradiation, a similar elimination or nucleation will occur in the reduced crystals of $Nb_{22}O_{54}$ or oxygen-excess crystals of $Nb_{12}O_{29}$ under certain circumstances dependent on oxygen pressure.

For the formation of the 'crystallographic shear' (CS) structure, Anderson & Hyde (1967) have proposed a model for the case of the one-dimensional CS structure in the ReO_3 structure. They thought that the CS plane would be created by aggregation of oxygen vacancies and subsequent collapse into dislocation loops since there is an energetic advantage for the crystals in a process that reduces the number of point defects by clustering into large extended defects, or Wadsley defects. For the case of the two-dimensional CS structure present in the block structure the situation might be somewhat different. In order to introduce one phase of the block structures into another, displacement of a significant amount of both cations and oxygen ions must be explained for the coherent intergrowth between them, as in the 'cooperative diffusion' proposed by Andersson & Wadsley (1966). Such a speculation is beyond the discussion of the present experiment but it can be said that displacement of the cations will be associated with the 'quasi-tetrahedral sites' proposed in this paper. For a fuller understanding of the mechanism of the phase transformation in the shear structure of the block structures, the presence of the point defect at the tetrahedral sites should be also taken into account.

One of us (S.I.) wishes to thank Professor J. M. Cowley for his continuous encouragement, and to acknowledge the support of a N.S.F. Area Development Grant in Solid State Science (No. GU3169). The other two authors are grateful to the remaining members of the Nb–O research group in the NIRIM for their continued interest in and suggestions for this work.

References

ALLPRESS, J. G. (1969). *J. Solid State Chem.* **1**, 66–81.
ALLPRESS, J. G. (1970). *J. Solid State Chem.* **2**, 78–93.
ALLPRESS, J. G. & ROTH, R. S. (1971). *J. Solid State Chem.* **3**, 209–216.
ANDERSON, J. S. (1970). *Problems of Nonstoichiometry*, Edited by A. RABENAU, pp. 17–27. Amsterdam: North-Holland.
ANDERSON, J. S. & HYDE, B. G. (1967). *J. Phys. Chem. Solids*, **28**, 1393–1408.
ANDERSON, J. S., BROWNE, J. M., CHEETHAN, A. K., VON DREELE, R., HUTCHISON, J. L., LINCOLN, F. J., BEVAN, D. J. M. & STREHLE, J. (1973). *Nature, Lond.* **243**, 81–83.
ANDERSSON, S. & WADSLEY, A. D. (1966). *Nature, Lond.* **211**, 581–583.

COWLEY, J. M. & IIJIMA, S. (1972). *Z. Naturforsch.* **27a**, 445–451.
GATEHOUSE, B. M. & WADSLEY, A. D. (1964). *Acta Cryst.* **17**, 1545–1554.
GRUEHN, R. & NORIN, R. (1967). *Z. anorg. allgem. Chem.* **355**, 176–181.
GRUEHN, R. & NORIN, R. (1969). *Z. anorg. allgem. Chem.* **367**, 209–218.
IIJIMA, S. (1973). *Acta Cryst.* A**29**, 18–24.
IIJIMA, S. & ALLPRESS, J. G. (1973). *J. Solid State Chem.* **7**, 94–105.
IIJIMA, S. & ALLPRESS, J. G. (1974*a*). *Acta Cryst.* A**30**, 22–29.
IIJIMA, S. & ALLPRESS, J. G. (1974*b*). *Acta Cryst.* A**30**, 29–36.
IIJIMA, S., KIMURA, S. & GOTO, M. (1973). *Acta Cryst.* A**29**, 632–636.
KIMURA, S. (1973). *J. Solid State Chem.* **6**, 438–449.
NIMMO, K. M. & ANDERSON, J. S. (1972). *J. Chem. Soc. Dalton*, pp. 2328–2337.
NORIN, R. (1963). *Acta Chem. Scand.* **17**, 1391–1404.
NORIN, R. (1965). *Acta Chem. Scand.* **20**, 871–880.
ROTH, R. S. & WADSLEY, A. D. (1965). *Acta Cryst.* **18**, 724–730.
SCHÄFER, H., BERGNER, D. & GRUEHN, R. (1969). *Z. anorg. allgem. Chem.* **365**, 31–50.
WADSLEY, A. D. & ANDERSSON, S. (1970). *Perspectives in Structural Chemistry*, Edited by J. D. DUNITZ and J. A. IBERS, Vol. 3. New York: John Wiley.

Acta Cryst. (1974). A**30**, 257

The Use of Symmetry with the Fast Fourier Algorithm

BY DAVID A. BANTZ AND MARTIN ZWICK

Department of Biophysics, The University of Chicago, Chicago, Illinois 60637, *U.S.A.*

(*Received* 9 *August* 1973; *accepted* 14 *September* 1973)

This paper presents an algorithm for making use of symmetry in the fast Fourier transform in a simple and general way which is applicable to nearly all space groups. This allows one to reduce storage requirements to approximately what is needed for an asymmetric unit of the electron-density function, and hence makes possible economical forward and reverse transforms of large unit cells in core.

Introduction

In recent years the 'Fast Fourier Transform' (FFT) of Cooley & Tukey (1965) has been increasingly applied to problems in crystallography and electron microscopy. A consideration limiting its use, however, has been the fact that, while Friedel symmetry may be conveniently incorporated into the algorithm, it has only recently been possible to make use of space-group symmetry to reduce storage and computing time requirements. The storage problem is more serious since it frequently happens, particularly for crystals of large biological molecules, that the available core storage is not sufficient to include the entire unit cell, which is what the fast Fourier algorithm normally requires. Exceeding the core limitations forces one to use a more complex and time-consuming form of the algorithm which uses tape or disk for storage (Gentleman & Sande, 1966; Brenner, 1968, 1972; Singleton, 1968; Hubbard & Quicksall, 1970). The net result of not using space-group symmetry and having to include the entire unit cell in the transform is to erode the savings possible with the FFT; indeed, for high-symmetry space groups, the fast Fourier method may not have a significant advantage over conventional algorithms, and may even be costlier. For these reasons, an approach which allows the FFT to make use of space-group symmetry is of some value, as this could provide the storage factor necessary to allow the computations to be done in-core.

We present such an approach. A method which bears some similarities to the procedures we set out here, has been proposed by Ten Eyck (1973), who has analyzed how the fast Fourier algorithm might be modified to include various possible symmetries. The present approach differs from Ten Eyck's in being simpler and more general since only standard, unmodified, fast Fourier subroutines are used. On the other hand, it suffers from the disadvantage of making full use of symmetry only for storage, but not for time reductions.

Procedure

For space-group symmetry with N general positions given by rotations and translations, S^j and $\mathbf{t}^j$, $j=1, \ldots, N$, the electron-density function and its transform have the symmetry,

$$\varrho(S^j\mathbf{x}+\mathbf{t}^j)=\varrho(\mathbf{x}) \tag{1}$$

and

$$F(\tilde{S}^j\mathbf{h})=\exp(-2\pi i\mathbf{h}\,.\,\mathbf{t}^j)F(\mathbf{h}) \tag{2}$$

since

$$\tilde{S}^j\mathbf{h}\,.\,\mathbf{x}=\mathbf{h}\,.\,S^j\mathbf{x}=\mathbf{h}\,.\,(\mathbf{x}^j-\mathbf{t}^j)\,. \tag{3}$$

Centering is included in these equations by operations of the form $[S^j,\mathbf{t}^j+\boldsymbol{\tau}]$ where $\boldsymbol{\tau}$ is the appropriate trans-